Flow : a study of electron transport through networks of interconnected nanoparticles

Blok, S.

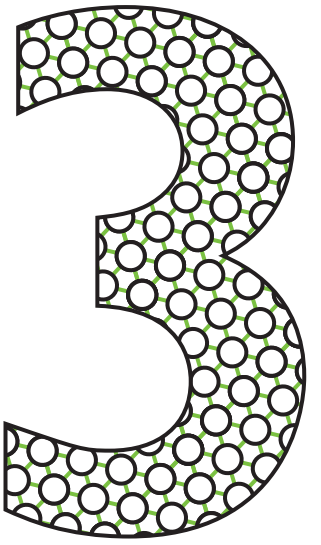

Cotunneling with energy dependent contact transmission

This chapter has been published as:
Inelastic cotunneling with energy-dependent contact transmission
S. Blok, R.R. Agundez Mojarro, L.A. Maduro, M. Blaauboer, S.J. van der Molen
Journal of Chemical Physics, 2016

3.1 Introduction

As discussed in chapter 2, at sufficiently low temperature and applied bias, electron transport through a gold nanoparticle array is expected to be dominated by higher order processes, specifically: multiple inelastic cotunneling. Multiple inelastic cotunneling involves two or more electrons that all contribute to the transport process. Since the intermediate states are energetically forbidden, this form of transport binds the fates of two or more electrons together in one transport event. In cotunneling, electrons are the ultimate party poopers; if one electron does not contribute to the event, none of the electrons will and transport does not occur. Since each single electron contribution is independent of the other, it can be easily seen that the resulting current scales with the single electron transmission probability to the N$^{\text{th}}$ power $I \propto \mathcal{T}^N$, where $N \geqslant 2$ is related to the amount of electrons involved[1,2]. This can also be seen in the previous chapter; in Eq. 2.7 the current scales with the conductance to the second power. Here, there are two electrons involved, and the conductance is proportional to the single electron transmission probability.

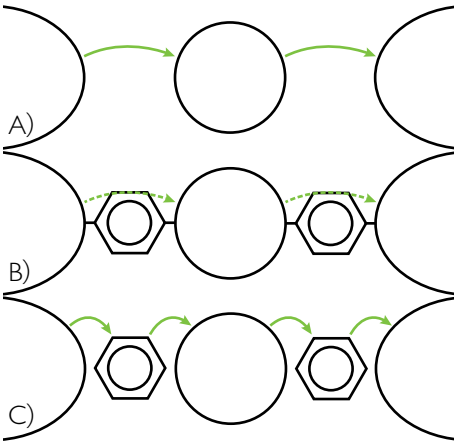

Fig. 3.1: Three approaches to the cotunneling problem. **A**: the original method developed by Nazarov *et al.*[3]. Here, the electrons tunnel through tunnel barriers with energy independent transmission probability in a single cotunneling process. **B**: electrons go from left to right via a single cotunneling process, but the transmission probability of the electrons depends on their incoming energy. **C**: an adaptation of the multiple cotunneling model[4]. Electrons go from the left lead to the right lead via a multiple cotunneling process through various virtual states. Since the molecules are modeled as single levels as opposed to the leads and nanoparticle, cotunneling through the molecules is elastic, whereas tunneling through the nanoparticle is inelastic.

Thus far, the resulting cotunneling current has only been calculated for systems in which the transmission probability is independent of energy. This assumption does not generally apply to molecules bridging between neighboring nanoparticles however, as molecular transmission functions can be strongly energy-dependent. Understanding the influence of the latter is not only of fundamental interest; it is also relevant for practical devices, since cotunneling can be utilized to enhance the signature of the molecules bridging[5] the nanoparticles in an array. If, for example, the bridges are formed by molecular switches, the ratio between the conductance in the 'on' and the 'off' state can be artificially increased. In this

chapter, we study the effect of an energy-dependent transmission function on transport between nanoparticles in the Coulomb blockade regime. We propose two methods (outlined in Fig. 3.1B,C) to tackle this problem.

3.2 THEORY OF COTUNNELING MECHANISMS

In this section we briefly review the mechanisms of inelastic cotunneling. Classically, when a system is Coulomb blockaded, no current is expected to flow. However, it was predicted [3] and found experimentally [6,7] that due to quantum corrections, this is not completely the case. The current flowing in the Coulomb blockade regime is due to the process of cotunneling [3]. Cotunneling is the simultaneous transfer of multiple electrons through energetically forbidden virtual states. The basic mechanism is as follows. Consider the device illustrated in Fig. 3.1A. Two leads connect to a charging island from either side through a tunnel barrier. An electron can temporarily hop from the left lead onto the charging island. The resulting virtual charge state is energetically forbidden, but temporarily allowed by the Heisenberg uncertainty relation. In this time window, an electron already residing on the island may hop onto the right lead. If these two processes occur within this time window, an electron has effectively been transferred from the left to the right lead. The reverse process (i.e. to the right lead) is also possible, but the symmetry between these processes is broken by applying a voltage bias. The final charge state of the island is equal to the initial charge state, complying with total energy conservation.

There are two different types of cotunneling; elastic and inelastic. Elastic cotunneling can only be observed at sufficiently low bias and temperature [6], compared to the quantum level spacing of the charging island. In an elastic cotunneling process, the electron hopping onto the charging island and the electron hopping off have the same energy. In inelastic cotunneling, this is not the case. This results in the charging island being left in an excited state after the process. The inelastic cotunneling current through a single junction as depicted in Fig. 3.1A can be written as [3]:

$$I = \frac{1}{6\pi^2} G_0 \mathcal{T}^2 \frac{(eV)^2 + (2\pi k_B T)^2}{E_C^2} V, \tag{3.1}$$

where $\mathcal{T}$ is the transmission probability of the tunnel barrier, $G_0 = {}^{2e^2}/_h$ is the conductance quantum, E_C is the charging energy of the island, T is the temperature, k_B is the Boltzmann constant, e is the elementary charge and V is the voltage across the junction. Since two barrier transmissions are needed for transport to occur, it makes intuitive sense that $I \propto \mathcal{T}^2$. However, in the derivation of Eq. 3.1, it has been assumed that the transmission probability of the tunnel barriers is independent of energy. While this is normally a reasonable assumption, it is not always the case. In this chapter, we will explore the possibility of an energy-dependent transmission function. In the next section we consider the case where the two leads are connected to the nanoparticle through molecules, as seen in Fig. 3.1B. The

contact transmission is then expected to become dependent on electron energy, assuming a Lorentzian lineshape.

3.3 Approach 1: Lorentzian transmission

In this section, we will assume that each of the two molecules involved in the cotunneling problem can be represented by a single level, symmetrically connected to a lead and the central nanoparticle (see Fig. 3.1B). Furthermore, we will suppose that transport through each molecule is coherent, such that the transmission function becomes Lorentzian with a width determined by the lead-molecule coupling[8]. Still, inelastic cotunneling behavior in the full molecule-nanoparticle-molecule system is to be derived by allowing for virtual excitations. More specifically, an electron in the lead, with an energy E_{L}, will temporarily take up a different energy, E_{S2}, within the nanoparticle. As a result, the exact energy of electron transmission through the molecule is somewhat ill-defined. To circumvent this problem, we will assume that any change of energy, related to the formation of a virtual state, happens inside the nanoparticle. In that case, the molecular transmission function depends only on the energy of the incoming electron. Summarizing, we assume that all virtual processes take place within the charging island, while transmission through the molecules can still be described by the Lorentzian functions in Eq. 3.2:

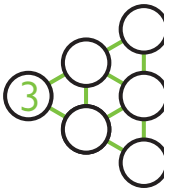

$$\begin{aligned}\mathcal{T}_{\mathrm{M1}}(E_{\mathrm{L}}) &= \frac{\Gamma^2}{\left(E_{\mathrm{L}} - \epsilon_{\mathrm{L}} - \eta_{\mathrm{L}} eV\right)^2 + \Gamma^2},\\ \mathcal{T}_{\mathrm{M2}}(E_{\mathrm{S1}}) &= \frac{\Gamma^2}{\left(E_{\mathrm{S1}} - \epsilon_{\mathrm{R}} - \eta_{\mathrm{R}} eV\right)^2 + \Gamma^2}.\end{aligned} \tag{3.2}$$

Here Γ is the half width half maximum of the Lorentzian which takes into account lead-molecule and molecule-nanoparticle coupling, ϵ_{R} and ϵ_{L} are the resonance energies of the molecular levels (we take $\epsilon_{\mathrm{R}} = \epsilon_{\mathrm{L}}$ in our calculations), $E_{\mathrm{L}}, E_{\mathrm{S1}}$ are the incoming electron energies and ηeV determines the shift of the level as an effect of the applied voltage. We take $\eta_{\mathrm{L(R)}} = (-)1/4$ in every calculation, implying an equal coupling to both the lead and the nanoparticle. Note that the maximum of the transmission function is taken to be unity.

To calculate the transition rate $\mathcal{R}$ from the initial state $|i\rangle$ to the final state $|f\rangle$, the Fermi Golden Rule[9] can be expanded in order to sum over all virtual states $|v\rangle$. Within this perturbative approach, the small parameter is the coupling between the nanoparticle and the two leads. The rate is given by:

$$\mathcal{R} = \frac{2\pi}{\hbar} \sum_{v} \left| \frac{\langle i|\hat{H}|v\rangle \ \langle v|\hat{H}|f\rangle}{E_v - E_{\mathrm{i}}} \right|^2 \delta(E_{\mathrm{i}} - E_{\mathrm{f}}), \tag{3.3}$$

where the delta function ensures total energy conservation. $\hat{H}$ is the same Hamiltonian as

used by Averin *et al.*, Eq. 1 [3], pragmatically extended to include energy-dependent transmission through the molecules. The initial, virtual and final states are the unperturbed eigenstates of the molecule-nanoparticle-molecule system. The process amplitude should scale with the lifetime of the virtual state which is inversely proportional to the energy difference between the initial and virtual states: $E_\mathrm{i} - E_v$. There are two different virtual states as can be seen in Fig. 3.2. Either an electron on the left lead tunnels through the molecule to the nanoparticle, or an electron first goes from the nanoparticle through the molecule to the right lead. These processes are complementary; if the former process causes the virtual state, the latter leads to the final state and vice versa. For a system depicted in Fig. 3.2 the expression for the rate $\mathcal{R}$ is given in Eq. 3.4.

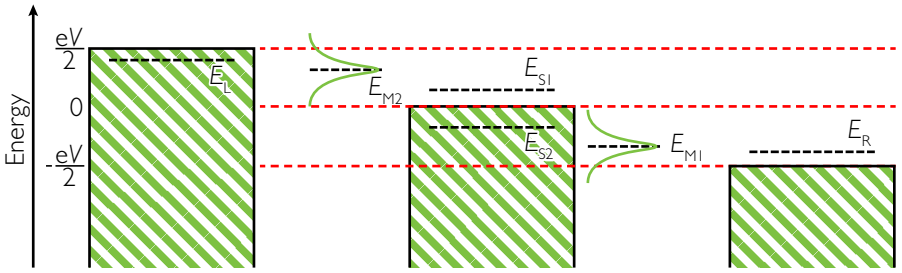

Fig. 3.2: Energy diagram of a charging island coupled to two leads with an applied bias voltage V. E_L and E_R are the electron energies of the left lead and the right lead, respectively. $E_{\mathrm{S}1}$ and $E_{\mathrm{S}1}$ are electron energies on the charging island.

$$\mathcal{R} = \frac{2\pi}{\hbar}\int_{\boldsymbol{E}} \mathcal{T}_{\mathrm{M}1}(E_\mathrm{L})\mathcal{T}_{\mathrm{M}2}(E_{\mathrm{S}1})\left[\frac{1}{\Delta E_{\mathrm{v}1}}+\frac{1}{\Delta E_{\mathrm{v}2}}\right]^2 \times F_\mathrm{FD}\delta(E_\mathrm{i}-E_\mathrm{f})\,\mathrm{d}E_\mathrm{L}\mathrm{d}E_\mathrm{R}\mathrm{d}E_{\mathrm{S}1}\mathrm{d}E_{\mathrm{S}2}, \quad (3.4)$$

$$F_\mathrm{FD} = f(E_\mathrm{L})\big[1-f(E_{\mathrm{S}2})\big]f(E_{\mathrm{S}1})\big[1-f(E_\mathrm{R})\big].$$

Here, the sum over virtual states has been replaced by an integral over all relevant energies. In Eq. 3.4, the matrix elements from Eq. 3.3 have been replaced by transmission probabilities $\mathcal{T}_{\mathrm{M}1}(E_\mathrm{L})$ and $\mathcal{T}_{\mathrm{M}2}(E_{\mathrm{S}1})$ analogously to Averin *et al.* [3], depending on the incoming electron energies E_l and $E_{\mathrm{S}1}$. It should be noted that these transmission functions are chosen for their general applicability and ease of understanding. The model presented here is not limited to these Lorentzian-shaped transmission functions, however and would work with other transmission functions as well. The energies E_L, $E_{\mathrm{S}2}$, E_R, $E_{\mathrm{S}1}$ are depicted

in Fig. 3.2. The energies ΔE_{v1} and ΔE_{v2} are defined as the energy differences between the initial and the first and second virtual state respectively. The occupation of states on the leads and nanoparticle are taken into account by their Fermi-Dirac distributions $f(E)$ (a derivation can be found in Appendix A).

Using Matlab we now calculate the cotunneling current $I(V)$ and differential conductance $^{dI}/_{dV}$ by solving Eq. 3.4 numerically for the system in Fig. 3.2. To test the validity of our approach, current versus voltage ($^{dI}/_{dV}$) was calculated for increasing coupling Γ for resonant transport ($\epsilon = \epsilon_L = \epsilon_R = 0$). As the coupling increases, the width of the transmission function (as seen in Eq. 3.2) increases. The consequence of this is that as Γ becomes larger, the cotunneling current should approach the constant transmission case. This can indeed be seen in Fig. 3.3. Here, Γ was varied from 3 meV to 1 eV and compared to the situation with constant transmission $\mathcal{T} = 1$, as derived by Averin *et al.*[3]. In Fig. 3.4 it can also be seen that as the coupling increases, the voltage at which the current starts to deviate from the constant-transmission case increases as well, as expected.

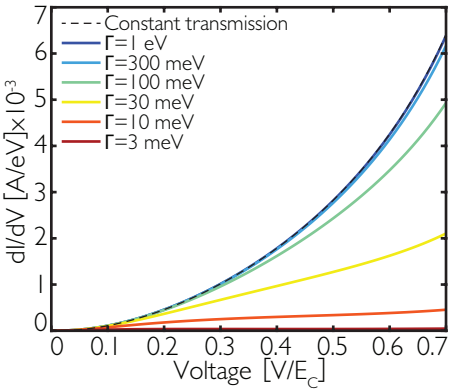

Fig. 3.3: Differential conductance ($^{dI}/_{dV}$) versus voltage curves for the system in Fig. 3.2 with varying Γ. It can be seen that as the coupling increases, the current approaches the constant transmission case, as is expected. The temperature is 116 K (10 $^{meV}/_{k_B}$), the charging energy E_C is 100 meV and we take $\epsilon_L = \epsilon_R = 0$ to ensure resonant transport through the molecules. The maximum value of the transmission function is unity in every case.

Next, we study the effects of molecular gating on the cotunneling current. Gating shifts the resonance position (ϵ_L and ϵ_R in Eq. 3.2) of the level. As a benchmark, let us first consider coherent transport through a single level connected to two leads, i.e. without Coulomb blockade. In that case, the maximal possible current can be calculated from the Landauer formula at 0 K.[10] (Eq. 3.5).

$$I = \frac{G_0}{e} \int_{-eV/2}^{eV/2} \mathcal{T}(E) \mathrm{d}E. \tag{3.5}$$

Clearly, the maximum possible current is the integral over the transmission function as $V \to \infty$. This (finite) number does not change if the peak of the Lorentzian is shifted and/or if the

temperature is changed to finite values.* In the cotunneling regime, the situation is different, as can be seen in Fig. 3.4. At low bias (for example at 0.2 $^{eV}/_{E_C}$), increasing $\epsilon = \epsilon_L = \epsilon_R$ away from zero, results in a decrease of the current indeed. However, at larger bias (for example at 0.45 $^{eV}/_{E_C}$), the current calculated for $\epsilon = 0$ meV is equal to the current found for $\epsilon = 5$ meV. In the $^{dI}/_{dV}$ (see Fig. 3.4B) at large bias (for example 0.7 $^{eV}/_{E_C}$), it can be seen that the differential conductance is larger for larger ϵ. This is never the case for systems without cotunneling, as the total current is only determined by the area of the transmission curve that is in the bias window. This suggests that cotunneling is selective for higher energy electrons, as long as the transmission function allows them to pass.

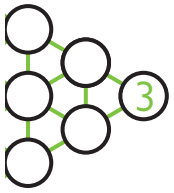

*As we saw in chapter 1, the maximum current is given by: $G_0\Gamma/e$

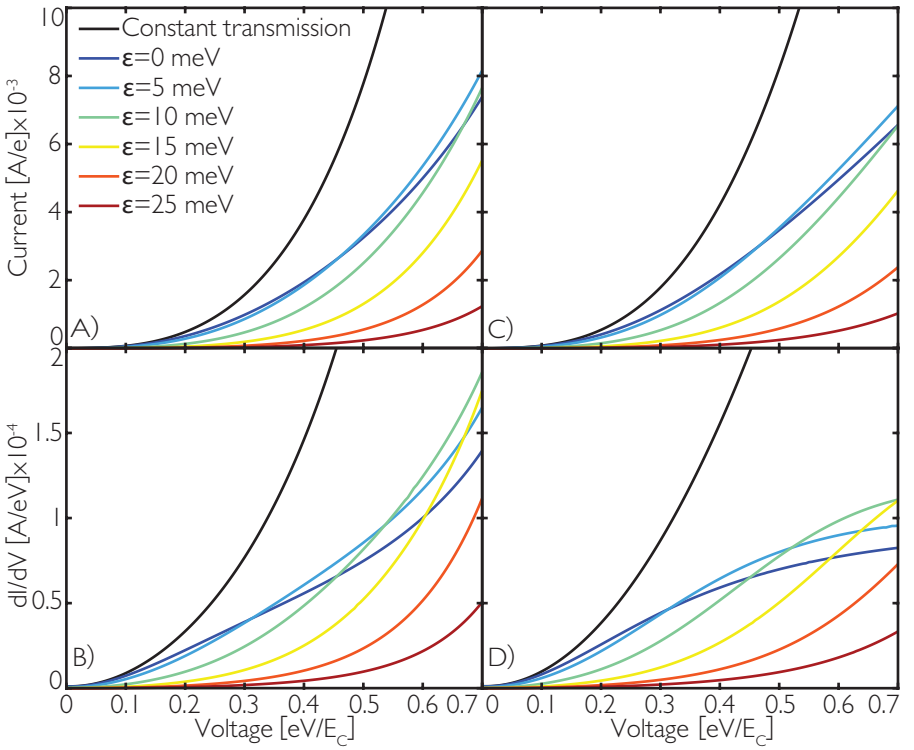

Fig. 3.4: Plots of current and differential conductance versus voltage for the system in Fig. 3.2, with ϵ varying from 0 to 25 meV (corresponding colors for all plots are denoted in A). The temperature is 12 K (1 $^{\text{meV}}/_{k_B}$), $\Gamma = 10$ meV and the charging energy $E_C = 100$ meV. The maximum transmission is unity in every case. The constant transmission curve (black) is added for reference. **A**: IV-plots. At low bias, the current decreases with increasing ϵ. However, as the bias gets larger, the difference decreases. At 0.45 $^{\text{eV}}/_{E_C}$, the curve for ϵ =0 meV crosses the curve for $\epsilon = 5$ meV; it even crosses the curve for ϵ =10 meV at 0.75 $^{\text{eV}}/_{E_C}$. **B**: dI/dV-curves derived from A, magnifying the trends observed in A. It can be seen that at 0.7 $^{\text{eV}}/_{E_C}$, the current increases most rapidly for $\epsilon = 10$ meV. **C**: IV-curves calculated upon approximating the denominator of eq. 3.4 by E_C. The crossings are still present, although somewhat shifted compared to A. **D**: dI/dV-curves derived from C. Again, crossings are found, but the shape of the individual curves differs from B. This can be expected, since the denominator of Eq. 3.4 as used in A and B diverges, in contrast to the case of C and D.

To explore possible explanations for this effect, we first note that the cotunneling current is inversely proportional to $(E_v - E_i)^2$ (or ΔE^2), as can be seen in Eq. 3.3. Hence,

electrons with a higher energy are energetically closer to the island charging energy. Thus they have a lower ΔE, increasing their transmission probability (see Eq. 3.4). To test if this phenomenon could lead to the crossing of curves as found in Fig. 3.4A and B, we have done a similar calculation but have replaced the $1/\Delta E^2$ by $1/E_C^2$. The results can be seen in Fig. 3.4C. We find that even though the crossings from Fig. 3.4C, D have changed their position, they have not disappeared. We conclude that the ΔE^2 in the denominator cannot be the principal source of the crossings.

A second explanation for the crossings can be seen in Eq. 3.4. Here, the electron energy not only appears due to the Heisenberg uncertainty relation, but also in the overall conservation of energy. The delta function relating the initial to the final energy in Eq. 3.4 can be written as $\delta(E_{S1} + E_R - E_L - E_{S1} - eV)$. This means that as the voltage increases, more cotunneling pathways are opened to allow transport. If the peak of the transmission function is at this higher energy, these pathways can also tunnel through the molecule, increasing the total current. If the peak of the transmission function lies at a lower energy, the high energy pathways are blocked by the molecule and can therefore not contribute to the current.

To experimentally test the predictions made here, a device that can gate molecules selectively is required, as a back-gate would also gate the nanoparticle. This is non-trivial, however. Fortunately, it may also be possible to test our model using molecular switches[11]. Diarylethylene based switches, for example, do not only change their total transmission, but also the position of the resonances[12]. Our predictions could be examined on nanoparticle arrays interlinked by molecular bridges, but this would also require our model to include percolation effects[11]. A more direct evaluation can be done on nanogap devices with a single nanoparticle placed in between the electrodes using dielectrophoresis[13,14]. The current within the Coulomb blockade regime should then be compared to the current outside of it for both states of the switch. This allows for a direct test of the validity of the model proposed above.

In this section, we have assumed that the molecular coupling to the leads and nanoparticle is strong. However, if this coupling is weak, the charging energy of the molecule itself could start to play a role too[15]. In that case, elastic transmission through the molecule is no longer possible and the only allowed pathway from the left lead to the right is through multiple cotunneling. The next section discusses this problem.

3.4 Approach 2: Multiple cotunneling

In this section, we study the system depicted in Fig. 3.1C and introduce a charging energy to each (weakly coupled) molecule in order to shift transport across them to the Coulomb blockade regime. To study transport in this regime, we propose a second model based on higher order cotunneling. In the previous section our model consisted of a second-order cotunneling event with coherent transport through the molecule. However, if the molecular energy levels are Coulomb blockaded, direct tunneling through the molecule is no longer allowed. Therefore transport across the molecules will only occur through cotunneling. In the system depicted in Fig. 3.1C, an electron can be transferred from the left lead to the right lead by a fourth-order cotunneling event, consisting of a collective hopping through four junctions: left lead-molecule, molecule-nanoparticle, nanoparticle-molecule and molecule-right lead.

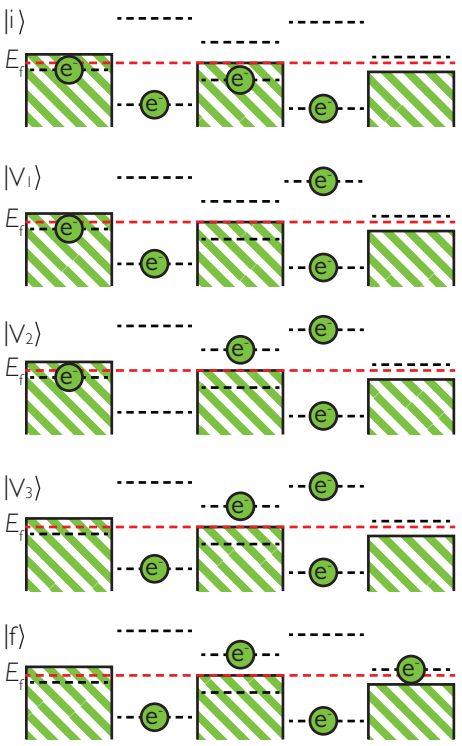

Fig. 3.5: The permutation $\{3, 2, 1, 4\}$ that contributes to the cotunneling current. Here, the process starts with an electron hopping from the nanoparticle to the right molecule, then from the left molecule to the nanoparticle, followed by an electron from the left lead to the left molecule and is completed by transfer from the right molecule to the right lead.

Transport across the nanoparticle is due to inelastic cotunneling. Since the molecules are modeled by a single level, transport across the molecule occurs through elastic cotunneling. Therefore, cotunneling transport in our system is of the fourth-order and consists of a collective combination of two elastic and one inelastic cotunneling events. In a second-order cotunneling event there are two possible hop permutations with distinct virtual states, as stated in the previous section. However, we now have four junctions, which means that there are $4!$ hop permutations, each with three virtual states. To calculate the total current in a four junction system, the contribution from each permutation needs to be taken into account. This can be done by considering the matrix

elements from Eq. 3.3 as:

$$M = \sum_{\{j_1,j_2,j_3,j_4\}} \prod_{k=1}^{3} \frac{\langle V_{k+1}| \hat{H} |V_k\rangle}{E_{\mathrm{V}_k} - E_{\mathrm{i}}} \langle V_1| H |i\rangle , \tag{3.6}$$

which sums over all possible permutations of the electron hops that yield the transport of an electron from the left lead to the right lead, e.g. $\{3, 2, 1, 4\}$ (see Fig. 3.5). The states $|V_k\rangle$ are the corresponding virtual states analogously to those defined in approach 1, used during the cotunneling process of each permutation, of which there are three per permutation. The Hamiltonian in Eq. 3.6 is the same as the one in Eq. 1 of Ref.[3], with two additional terms describing the two molecules (see below). The unperturbed eigenstates of the central molecule-nanoparticle-molecule region are represented, analogously to Ref.[3], as $|n_i\rangle$, with n_i ($i = \mathrm{M1}, \mathrm{NP}, \mathrm{M2}$) the number of electrons on molecule 1, the nanoparticle and molecule 2. The tunnel couplings between the left lead and left molecule, left molecule and nanoparticle, nanoparticle and right molecule and finally right molecule and right lead are the small parameters in this perturbative approach.

We model each molecule as a singly occupied energy level at the initial state as depicted in Fig. 3.5. This approximation is valid for a small bias if the energy level is in the Coulomb blockade regime, namely $\epsilon = -\frac{1}{2}E_{\mathrm{C,M}}$, where $E_{\mathrm{C,M}}$ is the Coulomb charging energy of the molecules. For the situation in Fig. 3.5, the initial energy for every permutation is $E_{\mathrm{i}} = E_{\mathrm{L}} + {}^{V}/_{2} + 2\epsilon + E_{\mathrm{S2}}$, and the final energy for every permutation is $E_{\mathrm{f}} = 2\epsilon + E_{\mathrm{S1}} + E_{\mathrm{R}} - {}^{V}/_{2}$. We can then write the total rate as a contribution of all possible initial and final energies, the sum of Eq. (3.3) for every set of energies, E_{L}, E_{R}, E_{S1} and E_{S2}. By converting the sum into an integral and the matrix elements $\langle V_{k+1}| \hat{H} |V_k\rangle$ in Eq. (3.6) into tunneling rates we write an explicit equation to calculate the cotunneling rate in our system[3,16] (see Appendix for details):

$$\begin{aligned}\mathcal{R} = &\frac{\hbar^3}{8\pi^3}\mathcal{T}_{\mathrm{M}}^4 \int_{\boldsymbol{E}} \left| \sum_{\{j_1,j_2,j_3,j_4\}} \prod_{k=1}^{3} \frac{1}{E_{\mathrm{V}_k} - E_{\mathrm{i}}} \right|^2 \\ &\times f_{\mathrm{FD}}\delta(E_{\mathrm{i}} - E_{\mathrm{f}})\mathrm{d}E_{\mathrm{L}}\mathrm{d}E_{\mathrm{R}}\mathrm{d}E_{\mathrm{S1}}dE_{\mathrm{S2}}.\end{aligned} \tag{3.7}$$

The Fermi distribution functions have been added to Eq. (3.7) to account for the probability of a state being empty or occupied, accordingly. The conservation of energy is taken into account by $\delta(E_{\mathrm{f}} - E_{\mathrm{i}})$. $\mathcal{T}_{\mathrm{M}}$ is the transmission probability for an electron going out of or into the molecule, $\mathcal{T}_{\mathrm{M}}$ takes the same role as $\mathcal{T}_{\mathrm{M1}}$ and $\mathcal{T}_{\mathrm{M2}}$ in Eq. 3.2, except that it is now assumed to be a constant (set to 1) independent of electron energy.

Moreover, the matrix element from Eq. 3.6 can be further simplified if we assume that the charging energy of the molecule and of the nanoparticle are larger than all other energies in the system. Interestingly, the energy independence of the matrix element results in the

multiple cotunneling behavior of the system reducing to singular cotunneling. This matrix element then becomes:

$$M = \frac{T_1^\dagger T_2^\dagger}{E_S}, \tag{3.8}$$

with $T_1^\dagger, T_2^\dagger$ taking into account the transmission probability to and from the molecules and E_S is a function of the charging energies of the molecules and nanoparticle. A complete derivation can be found in the appendix.

Using Matlab, we now calculate the cotunneling current ($I(V)$) by solving Eq. 3.7 numerically (see Fig. 3.6). We take the charging energy of the molecule to be ten times larger than the charging energy of the nanoparticle, $E_{C,M} = 10E_C$, together with a small bias voltage and $\epsilon = -\frac{1}{2}E_{C,M}$ ensures Coulomb blockade in the molecule and single occupancy. Analogously to our calculations in the previous section, we first calculate the current for varying molecular charging energies ($E_{C,M}$). From Eq. 3.7, we expect the current to decrease as the molecular charging energy increases. This can be seen in Fig. 3.6A.

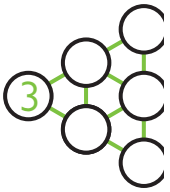

Since the amplitude of each pathway scales inversely with the product of all three energy differences ΔE_i, it can be expected that the total current should decrease with increasing molecular charging energy $E_{C,M}$. Furthermore, if the charging energies of the molecules and nanoparticle are much larger than both the electrostatic and thermal energies (eV and k_BT respectively) in the system, the shape of the I-V curves should not change when changing the charging energy. In Fig. 3.6B we have normalized each curve by the current at 70 meV. It can be seen that this moves the curves very close together, confirming our expectations. However, the rescaled curves are still not precisely identical.

If we now remove any thermal and electrostatic energy from the energy differences in the virtual pathways, we expect the IV-curves to fully overlap. Removing all energies except the charging energies in our calculation of the energy differences, we get the results shown in Fig. 3.6C. After normalization, these curves, displayed in Fig. 3.6D, lie fully on top of each other, as expected.

Interestingly, the calculations in this section predict that when a charging island is coupled to leads through Coulomb blockaded single levels, it is not possible to distinguish between multiple cotunneling and inelastic cotunneling with a constant transmission function (as derived by Averin *et al.* [3]). This holds for any system where transport across the system is through two instances of elastic cotunneling and one instance of inelastic cotunneling.

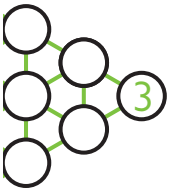

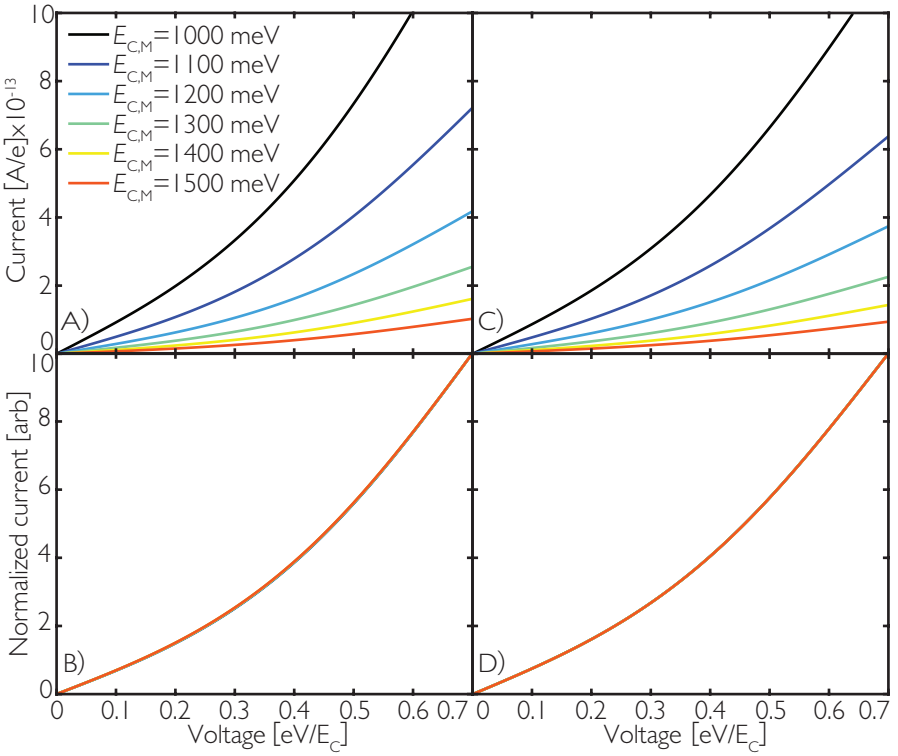

Fig. 3.6: IV curves for varying $E_{\mathrm{C,M}}$, calculated using Eq. 3.7. The temperature is set to 11.6 K, we take $E_{\mathrm{C}} = 100$ meV, and $E_{\mathrm{C,M}}$ is varied between 1 and 1.5 eV (see legend of A for the color coding, holding for all panels) **A**: IV-curves calculated. It can be seen that as $E_{\mathrm{C,M}}$ increases, the current decreases, as expected. **B**: Normalized IV-curves using the same parameters as in A, i.e. the current at $^{\mathrm{eV}}/_{E_{\mathrm{C}}} = 0.7$ has been set to unity for every curve. It can be seen that this normalization corrects for most of the differences due to variations in $E_{\mathrm{C,M}}$. However, it does not fully remove the variation between the curves. **C**: IV-curves calculated for varying $E_{\mathrm{C,M}}$, where all terms in the denominator other than the charging energies have been neglected. The result of this is that the sum over all virtual states is now a constant, independent of voltage. It can be seen that the total current is lower than in A. **D**: Normalized IV-curves using the same parameters as in C (normalization at $^{\mathrm{eV}}/_{E_{\mathrm{C}}} = 0.7$ again). Now the curves, calculated for different $E_{\mathrm{C,M}}$, lie exactly on top of one another.

3.5 Conclusion

We have explored two approaches to calculate inelastic cotunneling through a nanoparticle connected to two leads through molecules with energy-dependent transmission functions. In the first approach, the molecules are modeled as having single-level Lorentzian transmission functions. Interestingly, we find that at large applied bias, the current for systems with the molecular levels slightly off-resonant can be higher than for the case of resonant molecular levels. This remarkable behavior is a direct consequence of transport taking place via cotunneling. To test this prediction, a nanoparticle covered with molecules could be trapped in a nanogap using dielectrophoresis. Cotunneling transport in such a system is expected to deviate from results derived by Averin *et al.* [3]. In the second approach we model the molecules as Coulomb blockaded, so that transport across the molecules takes place through elastic cotunneling. We show that at low temperature and bias, the multiple cotunneling current should approach the expression for regular cotunneling. Our calculations support this by showing that the IV-curves are identical when normalized.

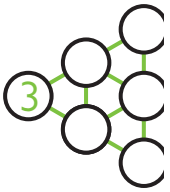

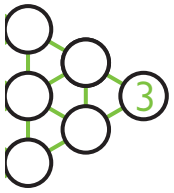

References

[1] T. Tran, I. Beloborodov, Jingshi Hu, X. Lin, T. Rosenbaum, and H. Jaeger. Sequential tunneling and inelastic cotunneling in nanoparticle arrays. *Physical Review B*, 78(7), 2008.

[2] J. F. Dayen, V. Faramarzi, M. Pauly, N. T. Kemp, M. Barbero, B. P. Pichon, H. Majjad, S. Begin-Colin, and B. Doudin. Nanotrench for nano and microparticle electrical interconnects. *Nanotechnology*, 21(33):335303, 2010.

[3] D. V. Averin and Yu V. Nazarov. Virtual electron diffusion during quantum tunneling of the electric charge. *Physics Review Letters*, 65(16):2446–2449, May 1990.

[4] T. Tran, I. Beloborodov, X. Lin, T. Bigioni, V. Vinokur, and H. Jaeger. Multiple cotunneling in large quantum dot arrays. *Physical Review Letters*, 95(7), August 2005.

[5] Jean-Francois Dayen, Edwin Devid, Mutta Venkata Kamalakar, Dmitry Golubev, Constant Guédon, Vina Faramarzi, Bernard Doudin, and Sense Jan van der Molen. Enhancing the Molecular Signature in Molecule-Nanoparticle Networks Via Inelastic Cotunneling. *Advanced Materials*, 25(3):400–404, jan 2013.

[6] A. E. Hanna, M. T. Tuominen, and M. Tinkham. Observation of Elastic Macroscopic Quantum Tunneling of the Charge Variable. *Physics Review Letters*, 68(21):3328, may 1992.

[7] L. J. Geerligs, D. V. Averin, and J. E. Mooij. Observation of macroscopic quantum tunneling through the coulomb energy barrier. *Physical review letters*, 65(24):3037, 1990.

[8] J.C. Cuevas and E. Scheer. *Molecular electronics, an introduction to theory and experiment*, volume 1. World Scientific Publishing Co., 2010. ISBN 981-4282-58-8.

[9] Paul A.M. Dirac. The quantum theory of the emission and absorption of radiation. *Royal Society London, Ser. A*, 114:243–265, 1927.

[10] R. Landauer. Spatial variation of currents and fields due to localized scatterers in metallic conduction. *IBM Journal of Research and Development*, 1(3):223–231, 1957.

[11] Sense Jan van der Molen, Jianhui Liao, Tibor Kudernac, Jon S. Agustsson, Laetitia Bernard, Michel Calame, Bart J. van Wees, Ben L. Feringa, and Christian Schönenberger. Light-controlled conductance switching of ordered Metal-Molecule-Metal devices. *Nano Letters*, 9(1):76–80, 2009.

[12] Colin Van Dyck, Victor Geskin, Auke J. Kronemeijer, Dago M. de Leeuw, and Jérôme Cornil. Impact of derivatization on electron transmission through dithienylethene-based photoswitches in molecular junctions. *Physical Chemistry Chemical Physics*, 15 (12):4392, 2013.

[13] Sanjeev Kumar, Seok-Hwang Yoon, and Gil-Ho Kim. Bridging the nanogap electrodes with gold nanoparticles using dielectrophoresis technique. *Current Applied Physics*, 9 (1):101 – 103, 2009.

[14] L. Bernard, M. Calame, S. J. van der Molen, J. Liao, and C. Schönenberger. Controlled formation of metallic nanowires via Au nanoparticle ac trapping. *Nanotechnology*, 18 (23):235202, June 2007.

[15] Bo Song, Dmitry A. Ryndyk, and Gianaurelio Cuniberti. Molecular junctions in the Coulomb blockade regime: Rectification and nesting. *Physical Review B*, 76(4), 2007.

[16] D. V. Averin and A. A. Odintsov. Macroscopic quantum tunneling of the electric charge in small tunnel junctions. *Physics Letters A*, 140(5), September 1989.